Toward the Implementation of an Anti-Windup Scheme for Vertical and Shape Control in the DIII-D Tokamak

E. Schuster, M.L. Walker, D.A. Humphreys, and M. Krstić

***Abstract*— The shape and vertical controller, which will be integrated in the future with control of plasma profiles, is the first step in the development of an integrated multivariable controller for the Advanced Tokamak (AT) operation mode in the DIII-D tokamak. In this work we focus on the constraints on actuator voltages and introduce an anti-windup scheme developed to accomodate the limitations of the plant in terms of access to the states, computational effort, and design complexity. This anti-windup augmentation is implemented for both the vertical loop (linear exponentially unstable plant) and the shape loop (nonlinear stable plant) in the DIII-D tokamak.**

I. Introduction

Demands for more varied shapes of the plasma and requirements for high performance regulation of the plasma boundary and internal profiles are the common denominator of the Advanced Tokamak (AT) operating mode in DIII-D. This operating mode requires multivariable control techniques to take into account the highly coupled influences of equilibrium shape, profile, and stability control. The initial step toward integrating multiple individual controls is the implementation of a multivariable shape and vertical controller for routine operational use. The long term goal is to integrate the shape and vertical control with control of plasma profiles such as pressure, radial E-field, and current profiles using feedback commands to actuators such as gas injectors, pumps, neutral beams (NB), electron cyclotron heating (ECH), and electron cyclotron current drive (ECCD).

The problem of vertical and shape control in tokamaks was and is still extensively studied in the fusion community. A recent summary of the existing work in the field can be found in [1]. Several solutions for the design of the nominal controller were proposed for different tokamaks using varied control techniques based on linearized models. However, only a few of them [2] take into account the control voltage constraint in the design of the nominal controller.

Several problems make practical implementation of shape and vertical position controllers on DIII-D challenging [3]. In this work we focus on the constraints on actuator voltages. This limitations imply that commands to shaping power supplies (choppers) often saturate, particularly with large or fast disturbances, causing unsatisfactory behavior and even loss of stability. The goal is the design of an anti-windup compensator that blends any given predesigned nominal controller, which is designed to fulfil some local (saturation is not considered) performance criterion, with a nonlinear feedback designed to guarantee stability and keep the nominal controll well behaved in the presence of input saturation but not necessarily tuned for local performance. The anti-windup augmentation must leave the nominal closed loop unmodified when no saturation is present.

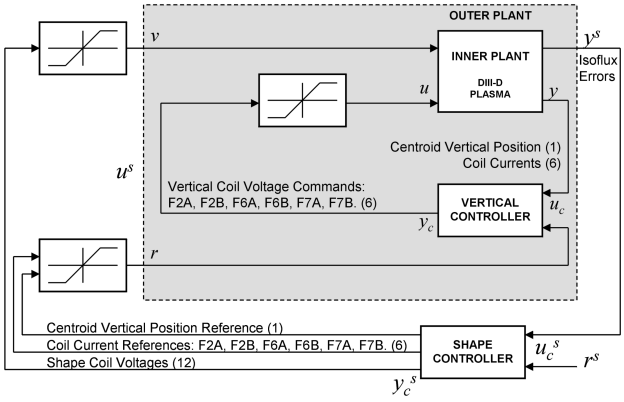

Fig. 1. Plant architecture.

The authors have previously approached the problem of plasma vertical position and shape control under actuation constraints in the DIII-D [4], [5] based on the ideas introduced in [6], [7]. In this work we introduce a refined anti-windup scheme based on the same ideas which allows us to overcome fundamental limitations of our systems in terms of access to the states and computational effort. In addition, the proposed scheme improves implementability, reducing design complexity, and performance, guaranteeing that the nominal loop is not modified when there is no input constraint.

The paper is organized as follows. Section II introduces the strategy used to control the shape and vertical position of the plasma in the DIII-D tokamak. Section III introduces the anti-windup scheme. Section IV focuses on the design of the inner loop while Section V focuses on the design of the outer loop. The conclusions are presented in Section VI.

II. Control Strategy

The time-scale properties of the system allow the separation of the vertical stabilization problem from the shape

This work was supported in part by grants from UCEI and NSF and by DoE contract number DE-AC03-99ER54463

E. Schuster and M. Krstić are with the Department of Mechanical and Aerospace Engineering, University of California at San Diego, 9500 Gilman Dr., La Jolla, CA 92093-0411 schuster@mae.ucsd.edu, krstic@ucsd.edu

M.L. Walker and D.A. Humphreys are with General Atomics, P.O. Box 85608, San Diego, CA 92186-5608 walker@fusion.gat.com, dave.humphreys@gat.com

control problem. These properties lead us to a multi-loop design as shown in Figure 1; the inner loop closed by the nominal vertical controller designed to control a linear exponentially unstable plant and the outer loop closed by the nominal shape controller designed to control a linear stabilized plant (saturation is not considered). Due to the constrained control, the nominal vertical controller may fail to stabilize the vertical position of the plasma inside the tokamak when large or fast disturbances are present or when the references coming from the shape controller change suddenly. The anti-windup synthesis problem is to find a nonlinear modification of the nominal vertical controller that prevents vertical instability and undesirable oscillations but leaves the inner loop unmodified when there is no input saturation. An anti-windup compensator is implemented for the given nominal vertical controller that together with conditioning algorithms for the reference signals guarantee stability of the linear exponentially unstable inner plant in the presence of actuactor saturation for all reference commands coming from the shape controller. Ensured the vertical stability of the plasma, a second anti-windup compensator is implemented to keep the given nominal shape controller well-behaved in the presence of rate and magnitude constraints at the input of the now augmented nonlinear stable outer plant.

III. Anti-Windup Compensator Fundamentals

For the presentation of the anti-windup problem we follow an approach similiar to the one introduced in [7]. We consider the plant

$$\begin{array}{rl} \dot{x} = & f(x,u) \\ y = & h(x,u) \end{array} \tag{1}$$

with control input $u \in \Re^m$, measurements $y \in \Re^p$ and states $x \in \Re^n$. In addition, we consider that a nominal controller with state $x_c \in \Re^{n_c}$, input $u_c \in \Re^p$, output $y_c \in \Re^m$ and reference $r \in \Re^p$,

$$\begin{array}{rl} \dot{x}_c = & g(x_c,u_c,r) \\ y_c = & k(x_c,u_c,r) \end{array} \tag{2}$$

has been already designed so that the closed loop system with interconnection conditions

$$u = y_c, \quad u_c = y \tag{3}$$

is (at least) locally well posed and stable. The controller performs well (at least) locally and succeeds regulating the plant to a desirable value x^* using the control value u^* asymptotically when $r = r^*$.

It is required that the nominal controller is used and unmodified on a prescribed, not necessarily bounded, neighborhood of (x^*, u^*) denoted by $\mathcal{F}$ where there is no input constraint. We assume there exist functions F and H and a point x_c^* such that

(a) $F(x,u) = f(x,u)$ and $H(x,u) = h(x,u)$ for all $(x,u) \in \mathcal{F}$

(b) $u^* = k(x_c^*, H(x^*,u^*), r^*)$

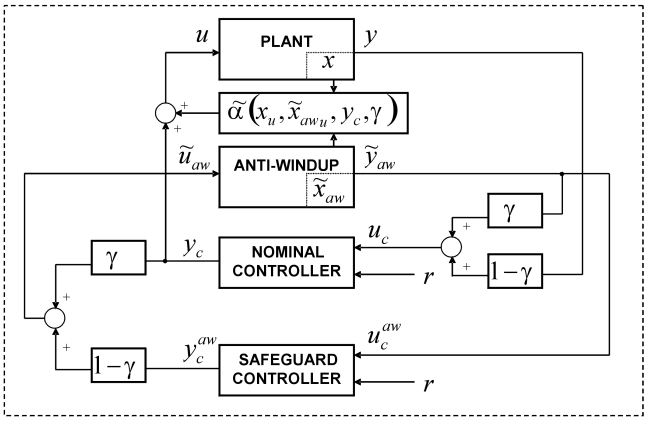

Fig. 2. Anti-windup scheme.

(c) the feedback interconnection of (2) with the system

$$\begin{array}{rl} \dot{x} = & F(x,u) \\ y = & H(x,u) \end{array} \tag{4}$$

is well-posed and locally Lipschitz and the point (x^*, x_c^*) is globally asymptotically stable.

Given that $\mathcal{F}$ is the region where there is no input constraint, it is natural to take the modified plant (4) as the input constraint free version of the original plant (1). Since in addition the nominal controller (2) is designed precisely for the input constraint free version of the original plant (modified plant (4)), the three assumptions are satisfied.

We propose the following anti-windup architecture:

$$\begin{array}{rl} \dot{\tilde{x}}_{aw} = & F(\tilde{x}_{aw}, \tilde{u}_{aw}) \\ \tilde{y}_{aw} = & H(\tilde{x}_{aw}, \tilde{u}_{aw}) \end{array} \tag{5}$$

with 'safeguard' controller (in the case of an unstable plant)

$$\begin{array}{rl} \dot{x}_c^{aw} = & g^{aw}(x_c^{aw}, u_c^{aw}, r^*) \\ y_c^{aw} = & k^{aw}(x_c^{aw}, u_c^{aw}, r^*) \end{array} \tag{6}$$

and interconnection conditions

$$u = y_c + \tilde{\alpha}(x_u, \tilde{x}_{aw_u}, y_c, \gamma), \tag{7}$$

$$u_c = (1-\gamma)y + \gamma \tilde{y}_{aw}, \tag{8}$$

$$\tilde{u}_{aw} = (1-\gamma)y_c^{aw} + \gamma y_c, \tag{9}$$

$$u_c^{aw} = \tilde{y}_{aw}, \tag{10}$$

where x_u and $\tilde{x}_{aw_u}$ represent the unstable modes of the state vectors x and $\tilde{x}_{aw}$ respectively. We are assuming that the state x, as well as the state $\tilde{x}_{aw}$, can be written separating unstable and stable modes, i.e.,

$$x = \begin{bmatrix} x_s \\ x_u \end{bmatrix}, \quad \tilde{x}_{aw} = \begin{bmatrix} \tilde{x}_{aw_s} \\ \tilde{x}_{aw_u} \end{bmatrix}, \tag{11}$$

and the plant (1) can be written as

$$\begin{array}{rl} \begin{bmatrix} \dot{x}_s \\ \dot{x}_u \end{bmatrix} = & \begin{bmatrix} f_s(x_s, x_u, u) \\ f_u(x_u, u) \end{bmatrix} \\ y = & h(x,u) \end{array} \tag{12}$$

where x_s is ISS with respect to x_u and u. Figure 2 shows a scheme of the anti-windup augmentation.

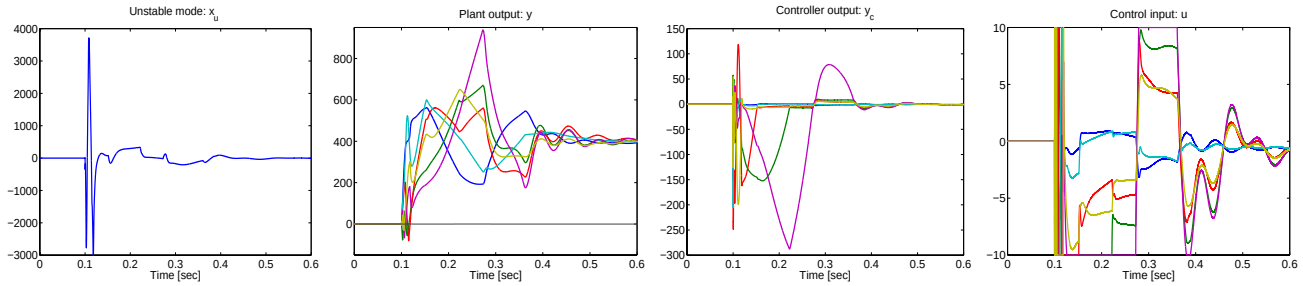

Fig. 3. System response without anti-windup to step changes of 400 Amps in r_{I_i}, for $i = 1, \ldots, m$, at $t = 0.1$ sec, $r_Z = 0$ and $v = 0$. The plasma growth rate is $\lambda = 500.7$.

The safeguard controller is designed with the only purpose of stabilizing the unstable modes of the antiwindup. There is no performance specification and usually we can achieve this goal with a relatively simple controller. We do not need any safeguard controller when the plant is stable. The switching function γ is defined as

$$\gamma = \begin{cases} 0 & (x,u) \in \mathcal{F} \\ 1 & \text{otherwise} \end{cases} \tag{13}$$

The function $\tilde{\alpha}$, inspired by [6], takes control of the plant when the unstable modes get close to the boundary of the controllable region (the region in which we have enough control authority to stabilize the plant even under the presence of input constraints),

$$\begin{aligned} \tilde{\alpha}(x_u, \tilde{x}_{aw_u}, y_c, \gamma) \quad = \quad & (1-\beta(x_u))(-y_c + \tilde{\alpha}_1(x_u)) \\ & +\beta(x_u)\gamma\tilde{\alpha}_2(x_u - \tilde{x}_{aw_u}). \end{aligned} \tag{14}$$

The function β is an indication of the position of the unstable modes within the controllable region, being one when the unstable modes are inside the "safe" region (a subset of the controllable region) and zero when the unstable modes are outside the "safe" region and approaching the boundary of the controllable region. We can note that

$$\beta = 1: \qquad \tilde{\alpha} = \gamma\tilde{\alpha}_2(x_u - \tilde{x}_{aw_u}), \tag{15}$$

$$\beta = 0: \qquad \tilde{\alpha} = -y_c + \tilde{\alpha}_1(x_u). \tag{16}$$

The controller $\tilde{\alpha}_1(x_u)$ is responsible for keeping the unstable mode x_u inside the controllable region. It is designed to make the point $x_u = x_u^*$ for the system

$$\dot{x}_u = f_u(x_u, \tilde{\alpha}_1(x_u)) \tag{17}$$

asymptotically stable within the controllable region, ensuring in addition that no trajectory starting within the controllable region leaves it. The controller $\tilde{\alpha}_2(x_u - \tilde{x}_{aw_u})$ is in charge of keeping the unstable mode x_u regulated to the anti-windup unstable mode x_{aw_u} when the nominal controler is fed by the anti-windup compensator during the constrained stage. It is important to note that when there is no input constraint ($\gamma = 0$) and the unstable mode is within the "safe" region ($\beta = 1$), the nominal feedback loop is not modified, i.e., $u = y_c$.

When $\gamma = 1$, the nominal controller is fed by the anti-windup compensator (unconstrained plant). In this way we keep the nominal controller well behaved. During the saturation stage, the controller $\tilde{\alpha}_2(x_u - \tilde{x}_{aw_u})$ is crucial. It must keep the unstable modes x_u always regulated to x_{aw_u} (which is driven by the nominal controller to its equilibrium value) to be able to return to the non-constrained stage. In addition, the controller $\tilde{\alpha}_1(x_u)$ must ensure that the unstable modes x_u do not escape the controllable region. When $\gamma = 0$, the nominal loop composed of the nominal controller and the plant is not modified. During this stage we can see the importance of the safeguard controller in stabilizing the anti-windup compensator.

This anti-windup scheme does not require the whole state x of the plant (we only need to measure or estimate the unstable modes x_u), does not modify the nominal feedback loop when there is no input constraint and the unstable mode is within the "safe" region, and simplifies the design of $\tilde{\alpha}$ requiring the stabilization of the unstable mode as its unique goal.

IV. Inner Loop

A. Plant Characteristics

The inner plant is linear but exponentially unstable with control input $u \in \Re^m$ ($m = 6$), measurements $y \in \Re^p$ ($p = 7$), and additional inputs $v \in \Re^q$ ($q = 12$) (more details can be found in [4]). We write the inner plant ($n \approx 50$) in state-space form,

$$\begin{aligned} \begin{bmatrix} \dot{x}_s \\ \dot{x}_u \end{bmatrix} = \dot{x} = \quad & Ax + B\text{sat}(u) + Ev \\ y = \quad & Cx + D\text{sat}(u) + Gv. \end{aligned} \tag{18}$$

Figure 3 shows the response of the closed loop without anti-windup compensator when r_{I_i}, for $i = 1, \ldots, m$, are step functions of magnitude equal to 400 Amps ($r = [r_I^T \quad r_Z]^T$). In this case we consider the saturation levels $M_i^{max} = M_i^{min} = M = 10V$, for $i = 1, \ldots, m$ and each input channel u_i evolves within these limits. It is possible to note the large excursions of the controller output y_c. These large oscillations can be also seen at the output y of the system, placing its response far from the desired performance. For step functions of magnitude higher or equal to 500 Amps the unstable mode x_u escapes the controllable region and the response diverges, i.e., stability is lost. These oscillations at the output of the controller must be eliminated so that stability can be guaranteed.

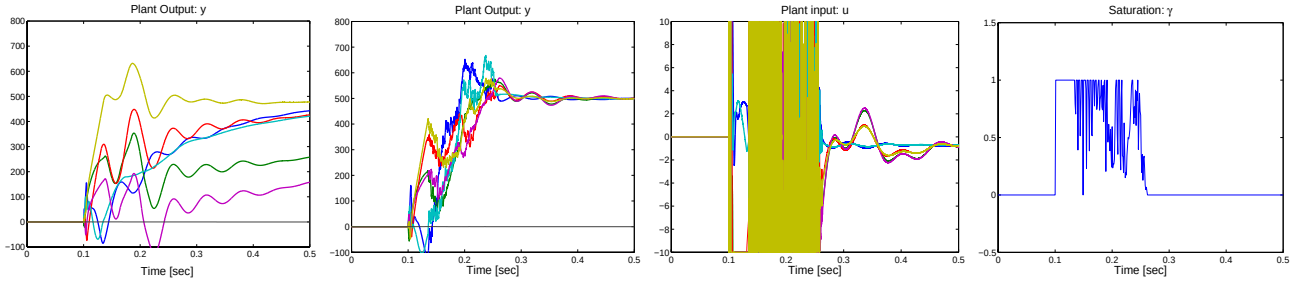

(a) (b) (c) (d)

Fig. 4. System response with anti-windup augmentation to step changes of 500 Amps in r_{I_i}, for $i = 1, \ldots, m$, at $t = 0.1$ sec, $r_Z = 0$ and $v = 0$ ($M_i^{max} = M_i^{min} = M = 10V$ for $i = 1, \ldots, m$). The plasma growth rate is $\lambda = 500.7$. The antiwindup compensator is implemented according to (19) (a) and (22) (b), (c), (d).

B. Antiwindup Implementation

The anti-windup scheme implemented in [4] is given by

$$\begin{array}{rcl} \dot{x}_{aw} = & Ax_{aw} + B[\text{sat}(y_c + \tilde{\alpha}) - y_c] \\ y_{aw} = & Cx_{aw} + D[\text{sat}(y_c + \tilde{\alpha}) - y_c], \end{array} \tag{19}$$

with interconnection conditions

$$u = y_c + \tilde{\alpha}, \quad u_c = y - y_{aw}. \tag{20}$$

Denoting $\hat{x}_u$ as the estimation of the unstable mode of the plant (no measurement is available), the proposed controller $\tilde{\alpha}$ was written as

$$\begin{array}{rcl} \tilde{\alpha}(\hat{x}_u, x_{aw_u}, y_c) & = & (\beta(\hat{x}_u) - 1)y_c \\ & & +(1 - \beta(\hat{x}_u))K_u\hat{x}_u + \beta(\hat{x}_u)K_u x_{aw_u}. \end{array} \tag{21}$$

Figure 4-a shows the simulation result for this scheme. As it was discussed in [4], the poor performance is due to the fact that the state x_{aw_s} is converging to zero in open loop. In this scheme, the nominal controller is fed by the the states $\tilde{x}_{aw} = x - x_{aw}$ of the unconstrained plant and for good performance it is required a fast convergence of these states to the states of the actual plant (of the states x_{aw} to zero) when there is no saturation. This is not the case in this application because the state x_{aw_s}, which is evolving in open loop, has very slow modes. This problem can be solved by a more complex design of the anti-windup compensator (19) as it was proposed in [4] or by a more complex design of the controller $\tilde{\alpha}$ as it is proposed in [6].

The anti-windup scheme proposed in this paper is given by

$$\begin{array}{rcl} \dot{\tilde{x}}_{aw} = & A\tilde{x}_{aw} + B\tilde{u}_{aw} \\ \tilde{y}_{aw} = & C\tilde{x}_{aw} + D\tilde{u}_{aw} \end{array} \tag{22}$$

with safeguard controller (6), and interconnection conditions (7)–(10). The saturation (switching) function γ is defined as

$$\gamma = \begin{cases} 1 & |u| > p_2 M \\ \frac{|u| - p_1 M}{(p_2 - p_1)M} & p_1 M < |u| < p_2 M \\ 0 & |u| < p_1 M \end{cases} \tag{23}$$

with $p_1 \leq 1$ and $p_2 \geq 1$. The function $\tilde{\alpha}$ takes control of the plant when the unstable modes get close to the boundary of the controllable region,

$$\begin{array}{rcl} \tilde{\alpha}(\hat{x}_u, \tilde{x}_{aw_u}, y_c, \gamma) & = & (\beta(\hat{x}_u) - 1)y_c \\ & & +(1 - \beta(\hat{x}_u))K_u\hat{x}_u + \beta(\hat{x}_u)\gamma K_u(\hat{x}_u - \tilde{x}_{aw_u}) \end{array} \tag{24}$$

Figures 4-b,c,d show the simulation result for this refined scheme. In Figure 4-b we can see that the performance was improved notably (compared to Figure 4-a) without increasing the complexity of the controller $\tilde{\alpha}$ and the antiwindup compensator. The only modification in the controller $\tilde{\alpha}$ is that we make it zero when there is no saturation ($\gamma = 0$) and the unstable mode is in the safe region ($\beta = 1$), in order to avoid any modification of the nominal feedback loop. Figures 4-c,d show the input of the plant and the saturation function γ respectively. A proper selection of the parameters p_1 and p_2 allows us to make use of all the available control as it is desired in this application to increase the response rate. It is posible to note that during the transient the actuators are saturating but stability is maintained. The function γ is responsible for this behavior, deciding which signal feeds the nominal controller — the output of the plant y or the output of the antiwindup compensator (unconstrained plant) $\tilde{y}_{aw}$. In terms of design complexity, the function γ is very easy to implement and the safeguard controller admits a very simple design due to the fact that its sole goal is the stabilization of the anti-windup compensator. In this application its design is simplified even more because there is only one unstable mode. Figure 5 illustrates the architecture of this refined anti-windup compensator for the inner loop.

V. Outer Loop

A. Signal Conditioning

The proposed scheme has been shown in nonlinear simulations to be very effective in guaranteeing stability of the inner loop in the presence of voltage saturation of the vertical coils. The scheme will be tested in experimental conditions. However, it is possible to anticipate at this stage the need for conditioning the signals coming from the shape controller. A watch-dog will monitor the additional input v and keep it from making the controllable region shrink below a prespecified minimum size and from leaving

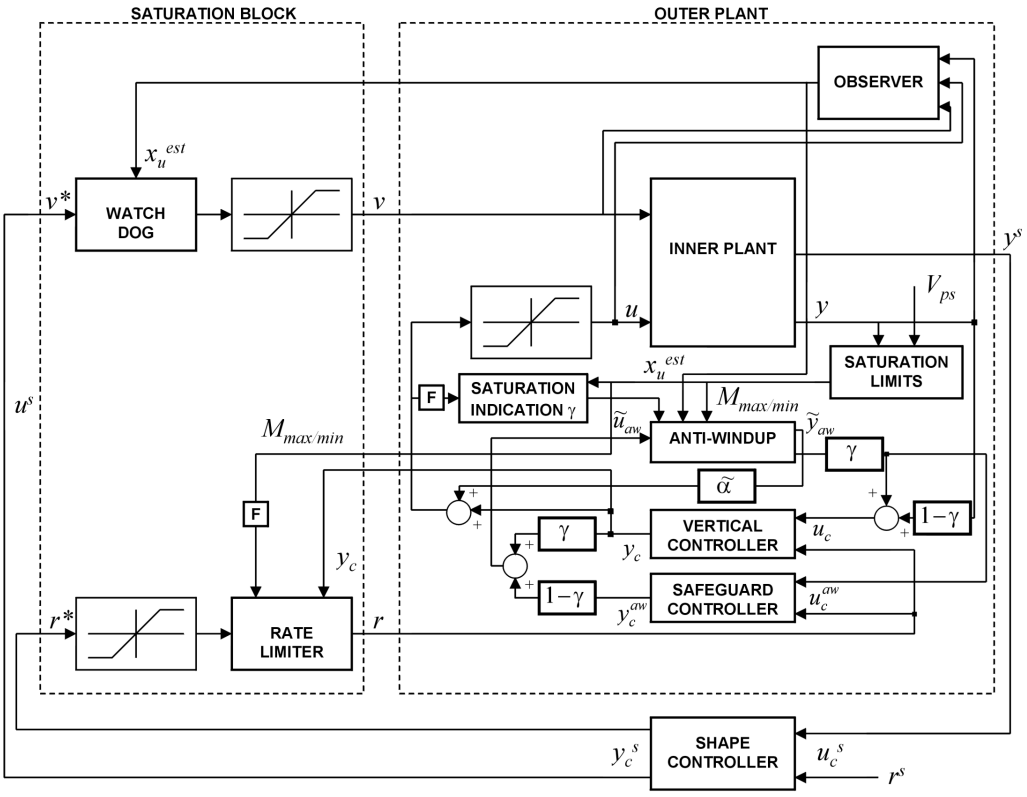

Fig. 5. Plant architecture with the inner loop anti-windup augmentation.

suddenly the unstable mode outside the controllable region. In addition, a rate limiter on r_I will be implemented to take into account the characteristic integration time of the coils.

The necessity of a similar anti-windup scheme for the outer loop is anticipated; not only due to the inherent limitations of its actuators but also due to the fact that the inner loop will modify, through the watch-dog and rate limiter, the control signals of the outer loop in order to preserve stability of the inner plant and improve performance. In this case we will deal with a stable (stabilized by the inner loop design) but nonlinear plant.

B. Plant Structure

The outer plant is the result of the anti-windup augmentation for the inner plant. The structure of our system is shown in Figure 5. The outer plant is the sum of the exponentially unstable inner plant, the nominal vertical controller, the state observer, and the inner loop anti-windup.

The structure of the plant shown in Figure 5 can be represented now in a more condensed way as it is shown in Figure 6. We can write the dynamics of the overall plant as (more detail can be found in [5])

$$\dot{x}^s = \begin{bmatrix} \dot{x}_p^s \\ \dot{x}_a^s \end{bmatrix} = \begin{bmatrix} f_1(x_p^s, h_2(x_a^s, u^s)) \\ f_2(x_a^s, u^s) \end{bmatrix} \equiv f(x^s, u^s) \quad (25)$$

$$y^s = h_1(x_p^s, h_2(x_a^s, u^s)) \equiv h(x^s, u^s). \quad (26)$$

Defining $\mathcal{F}$ as the set of points (x^s, u^s) satisfying $u^s = w^s$, we may take

$$F(x^s, u^s) \equiv \begin{bmatrix} f_1(x_p^s, u^s) \\ f_2(x_a^s, u^s) \end{bmatrix} \quad (27)$$

$$H(x^s, u^s) \equiv h_1(x_p^s, u^s), \quad (28)$$

which match $f(x^s, u^s)$ and $h(x^s, u^s)$ on $\mathcal{F}$.

C. Anti-windup Implementation

The antiwindup implemented in [5] is given by

$$\begin{aligned} \dot{x}_{aw}^s &= f(x^s, u^s) - F(x^s - x_{aw}^s, y_c^s) \\ y_{aw}^s &= h(x^s, u^s) - H(x^s - x_{aw}^s, y_c^s) \end{aligned} \quad (29)$$

and interconnection conditions

$$u^s = y_c^s + \tilde{\alpha}^s(x_{aw}^s) \quad (30)$$

$$u_c^s = y^s - y_{aw}^s, \quad (31)$$

where we can make $\tilde{\alpha}^s = 0$ in this case because we are dealing with a stable plant.

As it was discussed in [5], taking advantage of the stability properties of the plant it is possible to implement (29) replacing the state x^s by an estimation $\hat{x}^s$ obtained by an open-loop observer. However, in order to regulate fast the anti-windup state x_{aw}^s to zero, we may need a more complex design of the anti-windup compensator or the controller $\tilde{\alpha}^s$ (not $\tilde{\alpha}^s = 0$). Even succeeding in the design of this more complex anti-windup augmentation, a

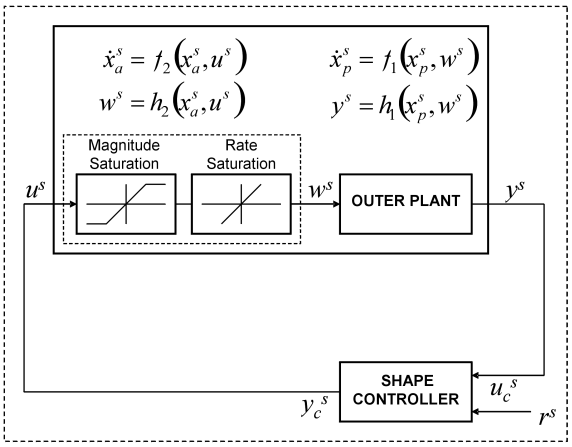

Fig. 6. Outer loop structure.

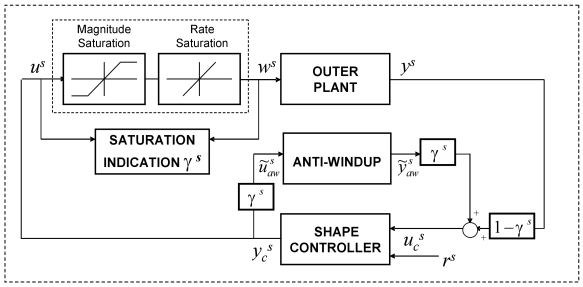

Fig. 7. Plant architecture with the outer loop anti-windup augmentation.

good performance of the scheme is not guaranteed because we would be regulating $\tilde{x}_{aw}^s$ to $\hat{x}^s$ and not to x^s as it is required to achieve the primary goal of the anti-windup: the preservation of the nominal feedback loop when there is no saturation.

The antiwindup proposed in this paper is given by

$$\begin{aligned} \dot{\tilde{x}}_{aw}^s &= F(\tilde{x}_{aw}^s, \tilde{u}_{aw}^s) \\ \tilde{y}_{aw}^s &= H(\tilde{x}_{aw}^s, \tilde{u}_{aw}^s) \end{aligned} \tag{32}$$

and interconnection conditions

$$u^s = y_c^s \tag{33}$$

$$u_c^s = (1-\gamma^s)y + \gamma^s \tilde{y}_{aw}^s, \tag{34}$$

$$\tilde{u}_{aw}^s = \gamma^s y_c^s. \tag{35}$$

where we adopt $\tilde{\alpha}^s = 0$ as our design because the plant is stable. For the same reason, there is no need to implement a safeguard controller. The last interconnection condition can be changed to $\tilde{u}_{aw}^s = y_c^s$ if we prefer to have the anti-windup compensator driven by the nominal controller when there is no saturation ($\gamma^s = 0$) instead of evolving in open loop. The switching function γ^s is defined as

$$\gamma^s = \begin{cases} 0 & \text{if } w^s = u^s \\ 1 & \text{otherwise.} \end{cases} \tag{36}$$

Figure 7 illustrates the architecture of the anti-windup augmentation for the outer loop. Comparing (29) and (32), we can note that the design has been simplified considerably. The refined anti-windup scheme (32) does not require access to the state of the plant, does not modify the nominal feedback loop when there is no saturation, simplifies the design not requiring a complex controller $\tilde{\alpha}^s$, and reduces the computational effort avoiding the computation of $f()$ and $h()$.

VI. Conclusions

The refined anti-windup augmentation scheme introduced in this paper proves in simulations to be very effective in accomodating the limitations of our plant in terms of access to the states, computational effort and design complexity. Simulation studies show that the proposed anti-windup scheme can perform equally or better than other previous schemes with a simpler design and an architecture more suitable for direct implementation.

It is important to emphasize that this scheme was developed seeking the reduction of implementation requirements. It is not the goal of the scheme to outperform similar anti-windup algorithms. Keeping an acceptable level of performance, we aim at reducing implementation complexity. The results are key for the implementation of an anti-windup scheme in the DIII-D tokamak; especially for the outer loop, where we have a high order nonlinear plant whose states are not all accessible.

The proposed scheme shows promise but a serious stability analysis in systems affected by disturbances would be helpful to assess the validity and scope of the sheme.

References

[1] R. Albanese and G. Ambrosino, "Current, position and shape control of tokamak plasmas: A literature review," *Proceedings of the 2000 IEEE International Conference on Control Applications*, Anchorage, Alaska, USA, pp. 412-18, September 2000.

[2] L. Scibile and B. Kouvaritakis, "A discrete adaptive near-time optimum control for the plasma vertical position in a tokamak," *IEEE Transactions on control systems technology*, Vol.9, no.1, p. 148, January 2001.

[3] M.L. Walker, D.A. Humphreys and E. Schuster, "Some nonlinear Controls for Nonlinear Processes in the DIII-D Tokamak," *Proceedings of the 2003 Conference on Decision and Control*, Maui, Hawaii, USA, December 2003.

[4] E. Schuster, M. L. Walker, D. A. Humphreys and M. Krstic, "Plasma Vertical Stabilization in Presence of Coil Voltage Saturation in the DIII-D Tokamak," *Proceedings of the 2003 American Control Conference*, Denver, Colorado, USA, June 2003.

[5] E. Schuster, M. L. Walker, D. A. Humphreys and M. Krstic, "Anti-windup Scheme for Plasma Shape Control with Rate and Magnitude Actuation Constraints in the DIII-D Tokamak," *Proceedings of the 2003 Conference on Decision and Control*, Maui, Hawaii, USA, December 2003.

[6] A. R. Teel, "Anti-Windup for Exponentially Unstable Linear Systems," *International Journal of Robust and Nonlinear Control*, vol.9, pp. 701-716, 1999.

[7] A. R. Teel, "Dynamic anti-windup for nonlinear control systems," submitted to the *IEEE Transaction on Automatic Control*.